Enhancement of thermoelectric efficiency in type-VIII clathrate $Ba_8Ga_{16}Sn_{30}$ by Al substitution for Ga

Shukang Deng, Yuta Saiga, Koichiro Suekuni, and Toshiro Takabatake[a)]
Department of Quantum Matter, ADSM and IAMR, Hiroshima University, Higashi-Hiroshima 739-8530, Japan

(Received 11 May 2010; accepted 21 August 2010; published online 7 October 2010)

Single-crystalline samples of type-VIII clathrate $Ba_8Ga_{16-x}Al_xSn_{30}$ ($0 \le x \le 12$) were grown from Sn flux to characterize the structural and thermoelectric properties from 300 to 600 K. The lattice parameter increases by 0.5% as x is increased to 10.5 whose value is the solubility limit of Al. The Seebeck coefficients of all samples are largely negative and the absolute values increase to approximately 300 μV/K on heating to 600 K. This large thermopower coexists with the metallic behavior in the electrical resistivity. The values of resistivity for $1 \le x \le 6$ at 300 K are in the range 3.3–3.8 mΩ cm which is 70% of that for $x=0$. As a result, the power factor for $x=4$ and 6 has a rather large maximum of 1.83×10^{-3} W/m K^2 at 480 K. The thermal conductivity stays at a low level of 0.72 W/mK up to 480 K, and the sample with $x=6$ reaches a ZT value of 1.2 at 500 K.
 [doi:10.1063/1.3490776]

I. INTRODUCTION

Over the last two decades, "caged" thermoelectric (TE) materials such as clathrates and filled skutterudites have attracted much attention due to their good combinations of high Seebeck coefficient α, low thermal conductivity κ, and low electrical resistivity ρ. In fact, some of the caged materials have large TE figure of merit defined as $ZT=\alpha^2T/\kappa\rho$, whose values at high temperatures are equivalent to state of the art materials.[1–4] Recently, a large number of investigations have been performed on type-I clathrates with the chemical formula of $II_8III_{16}IV_{30}$, where II=Ba, Sr, and Eu, III=Al, Ga, and In, and IV=Ge, Si, and Sn.[1–15] The unit cell of type-I clathrate consists of two kinds of cages; two dodecahedra and six tetrakaidecahedra formed by group IV and III elements. Alkaline-earth atoms in the cages donate electrons to framework host atoms so that the compound can be considered consisting of positively charged guest ions and negatively charged host cages.[9] Some (or all) of the electrons donated by the guest atoms can be accommodated as lone pairs formed in the cage structure through the group III element. The low κ at low temperatures is thought to be due to the phonon scattering by the local vibration of the guest atoms in the anharmonic potential.[1,5]

The type-VIII clathrate has the same chemical formula with the type-I clathrate, but the guest atoms are encapsulated in only one kind of polyhedral cage composed of 23 framework atoms.[16] The cage atoms occupy four sites as is shown in Fig. 1. As for type-VIII clathrates, only four compounds are known; $Sr_8Ga_{16-x}Al_xGe_{30}$ for $6 \le x \le 10$,[17] $Sr_8Ga_{16-x}Al_xSi_{30}$ for $8 \le x \le 10$,[18] $Ba_8Ga_{16}Sn_{30}$,[2,19–22] and $Eu_8Ga_{16}Ge_{30}$.[6,23,24] In type-VIII $Ba_8Ga_{16}Sn_{30}$, the atomic displacement parameters (ADP) of Ga/Sn are approximately twice that for Ga/Ge in type-I clathrate $Sr_8Ga_{16}Ge_{30}$, and the eight Ba atoms show a relatively large ADP.[21] For the lattice thermal conductivity, a small value of 1.1 W/mK was reported at room temperature.[22] Moreover, the carrier type can be tuned by slight deviation of the ratio of Ga/Sn from the ideal value of 16/30; excess of Ga leads to p-type conduction and excess of Sn leads to n-type conduction.[19,20] Previous papers on this system reported the TE properties at temperatures only below 300 K.[19–22]

In the present work, we address the properties of single-crystalline samples of $Ba_8Ga_{16-x}Al_xSn_{30}$ ($0 \le x \le 12$) at temperatures from 300 to 600 K. In analogy with the systems of $Sr_8Ga_{16-x}Al_xGe_{30}$ and $Sr_8Ga_{16-x}Al_xSi_{30}$,[17,20] it was expected that the substitution of a light element Al for Ga of the same III group may enhance the carrier mobility but not change the carrier density.

II. EXPERIMENTAL

Single-crystalline samples of $Ba_8Ga_{16-x}Al_xSn_{30}$ were prepared by Sn-flux method. High purity elements were mixed in an atomic ratio of Ba:Ga:Al:Sn=8:16−x:x:50 ($0 \le x \le 12$) in an argon atmosphere glovebox. The mixture

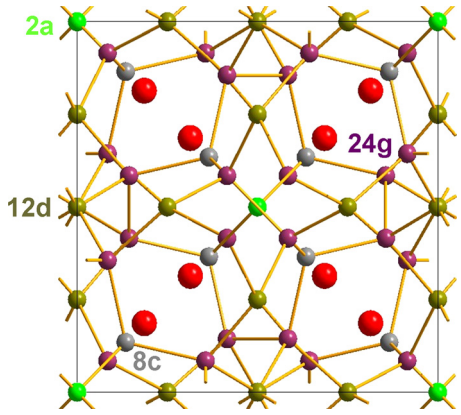

FIG. 1. (Color online) Unit cell of type-VIII clathrate $Ba_8Ga_{16}Sn_{30}$ viewed along the [100] direction. The large circles denote guest Ba atoms and small circles denote cage atoms of Ga and Sn.

[a)]Electronic mail: takaba@hiroshima-u.ac.jp.

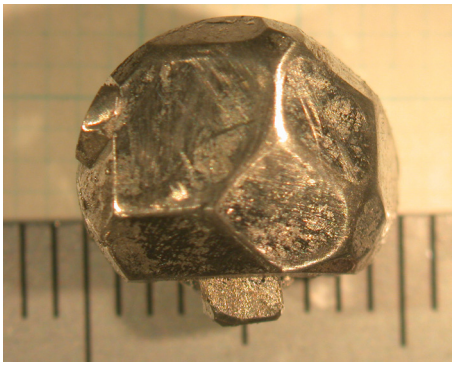

FIG. 2. (Color online) As grown single crystal of type-VIII clathrate $Ba_8Ga_{10}Al_6Sn_{30}$.

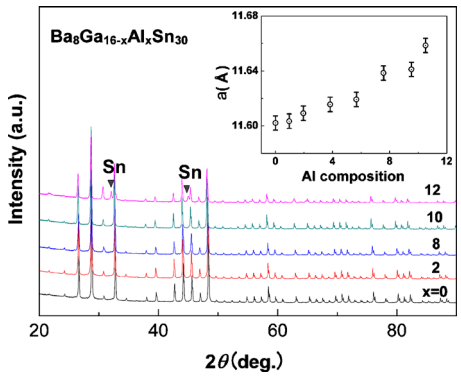

FIG. 3. (Color online) Powder XRD patterns for $Ba_8Ga_{16-x}Al_xSn_{30}$ samples taken with Cu $K\alpha$ radiation at room temperature. The inset shows the lattice parameter as a function of Al composition of the crystals.

sealed in an evacuated quartz tube was heated slowly to 763 K and soaked for 10 h, and then slowly cooled over 50 h to 663 K. The quartz tube was removed from the furnace at 663 K. Well-shaped crystals were separated from the molten Sn solvent by centrifuging. The constituent phase was characterized by powder x-ray diffraction (XRD, Rigaku Ultima IV), and the elemental compositions were determined by wavelength dispersive electron-probe microanalysis (EPMA, JEOL JXA-8200). The melting point of the sample was determined by differential thermal analysis (DTA, Bruker TG-DTA2000SA). Electrical resistivity and Seebeck coefficient were measured in a vacuum, respectively, by the standard dc four-probe method and the differential method from 300 to 600 K. The Hall coefficient R_H was measured at room temperature by a dc method in a magnetic field of 1 T. The temperature dependence of thermal conductivity was calculated via the equation $\kappa = DdC_p$, where D is the thermal diffusivity measured in a vacuum by a laser-flash method, d is the density, and C_p is the specific heat that was measured with a differential scanning calorimeter.

III. RESULTS AND DISCUSSION

A. Compositions and lattice parameters

Single-crystalline samples of approximately 5 mm in diameter were obtained for the Al starting composition $x < 10$. As for an example, the as grown crystal of $x=6$ has a shiny metallic luster as shown in Fig. 2. For $x=10$ and 12, however, the maximum crystal size was only 3 mm in diameter. After the sample with $x=12$ was exposed to the air, the surface easily changed from a shiny luster to an ash color.

The crystal compositions, whose values are the average over eight regions, are close to the starting compositions in the samples with $x \leq 10$. The total content of Ga and Al is less than the ideal composition of 16, and that of Sn is more than their ideal composition of 30. The Al composition in the sample with $x=12$ is largely reduced to 10.5, whose value is considered to be the solubility limit of Al in this system.

Figure 3 displays the XRD patterns for selected samples $Ba_8Ga_{16-x}Al_xSn_{30}$. All the patterns of samples with $x \leq 10$ are indexed by the type-VIII clathrate structure with space group $I\bar{4}3m$. For the sample with $x=12$, however, there are additional intensities at $2\theta = 32.0°$ and 44.3° which are attributed to Sn impurity. With the increase in x, the peak positions of the major phase shift to lower angles. This indicates that the lattice parameter increases with x due to the larger atomic radius of Al than Ga. In fact, as shown in the inset of Fig. 3, the lattice parameter increases almost linearly by 0.5% as the crystal composition of Al is increased to 10.5. The crystal compositions and lattice parameter a at room temperature are summarized in Table I.

The melting points of samples with $x=0$ and 6 were determined as 514 °C and 516 °C, respectively, from the endothermic peak of the DTA curves. This means no

TABLE I. Crystal compositions, lattice parameter a, Hall coefficient R_H, carrier density n, and carrier mobility μ_H at room temperature for $Ba_8Ga_{16-x}Al_xSn_{30}$ samples. Starting compositions Ba:Ga:Al:Sn are $8:(16-x):x:50$.

Sample x	Crystal composition					Lattice parameter a (Å)	Carrier density n (10^{19}/cm^3)	Hall coefficient R_H (cm^3/C)	Carrier mobility μ_H (cm^2/V s)
	Ba	Ga	Al	Sn	Ga+Al+Sn				
0	7.96	15.9	0	30.1	46.0	11.602(1)	4.23	−0.146	27.8
1	7.90	15.0	0.96	30.2	46.1	11.604(1)	⋯	⋯	⋯
2	7.97	13.9	1.95	30.2	46.0	11.609(1)	3.94	−0.157	45.4
4	7.97	12.0	3.83	30.2	46.0	11.612(1)	⋯	⋯	⋯
6	8.02	10.1	5.67	30.2	46.0	11.619(1)	4.62	−0.134	40.3
8	8.00	8.19	7.57	30.2	46.0	11.639(1)	4.51	−0.137	33.1
10	7.98	6.21	9.53	30.3	46.0	11.641(1)	⋯	⋯	⋯
12	7.99	5.23	10.5	30.3	46.0	11.659(1)	⋯	⋯	⋯

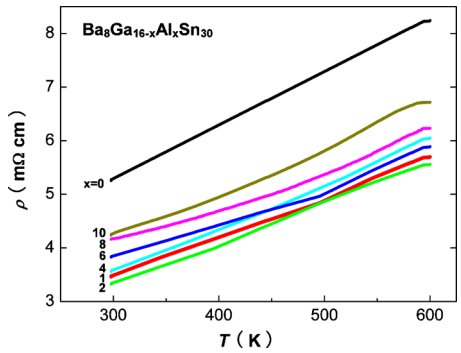

FIG. 4. (Color online) Temperature dependence of electrical resitivity ρ for type-VIII clathrate $Ba_8Ga_{16-x}Al_xSn_{30}$.

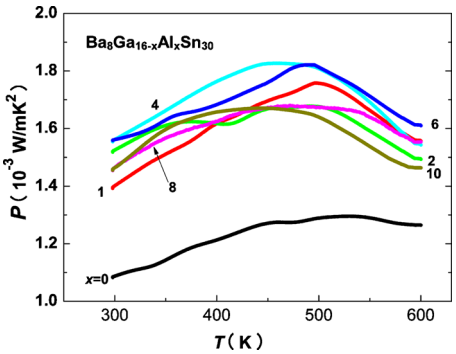

FIG. 6. (Color online) Temperature dependence of power factor P for type-VIII clathrate $Ba_8Ga_{16-x}Al_xSn_{30}$.

significant effect of Al substitution on the melting point of this system.

B. Electrical transport properties

Figure 4 shows the temperature dependence of electrical resistivity ρ for $Ba_8Ga_{16-x}Al_xSn_{30}$. For all samples, $\rho(T)$ increases monotonically in parallel with each other as the temperature is increased from 300 to 600 K. On going from $x=0$ to $x=2$, $\rho(T=300\ \text{K})$ decreases from 5.3 to 3.3 $\text{m}\Omega\,\text{cm}$, and then gradually increases to 4.2 $\text{m}\Omega\,\text{cm}$ with further increase in x to 10. To understand this unusual x dependence of $\rho(T)$, we measured the Hall coefficient at room temperature. As shown in Table I, all samples have negative Hall coefficient. The n-type nature of dominant carriers is related to the composition ratio of (Ga+Al)/Sn smaller than the ideal value of 16/30 as denoted in Table I. The carrier density is essentially constant at $4-5\times10^{19}/\text{cm}^3$ for $0\leq x\leq 8$, indicating that the conduction band structure is kept intact by the substitution. The rather low carrier density in this series of samples can be attributed to the absence of vacancy on the framework. In fact, the actual total compositions of framework atoms are nearly equal to 46 as listed in Table I. Using the value of ρ and R_H at 300 K, the carrier mobility was calculated as $\mu_H=|R_H|/\rho$. The carrier mobility largely increases as x is increased from 0 to 2, which may give rise to the initial reduction in ρ with x.

Figure 5 shows the Seebeck coefficient α of $Ba_8Ga_{16-x}Al_xSn_{30}$ as a function of temperature over the range 300–600 K. For all samples, α is largely negative in consistent with the negative sign of R_H. At 600 K, $|\alpha|$ first decreases on going from $x=0$ to 2, then increases on going from $x=2$ to 10. It is noteworthy that this sequence in $|\alpha(T=600\ \text{K})|$ with x is almost the same that in $\rho(T=600\ \text{K})$. The decrease in $|\alpha|$ with x up to $x=2$ can be attributed to the reduction in carrier effective mass, which is consistent with the higher mobility of carriers for $x=1$ and 2 than for others as discussed above.

Figure 6 displays the power factor $P=\alpha^2/\rho$. For the samples for $2\leq x\leq 6$, the power factor is enhanced distinctly compared with that for $x=0$ due to the reduced value of ρ. For the samples with $x=4$ and 6, the largest power factor is $1.83\times10^{-3}\ \text{W/m K}^2$ at 480 K, whose value is enhanced by 41% compared with the sample with $x=0$.

C. Thermal properties and figure of merit *ZT*

The temperature dependent thermal diffusivity of the samples with $x=0$, 4, 6, and 8 was measured by the laser-flash method. The data for other samples could not be obtained because the size of single crystals was smaller than the required size of 6 mm in diameter. Figure 7 shows the data of thermal conductivity κ from 300 to 600 K. The values of κ are 0.72–0.80 W/mK at 300 K and almost invariant with temperature up to 480 K. The marked increase in κ at higher temperatures can be attributed to the bipolar effect.[25] Such an effect becomes significant at high temperatures when thermally excited p-type carriers coexist with n-type carriers. Using the measured values of α, ρ, and κ, the ZT was cal-

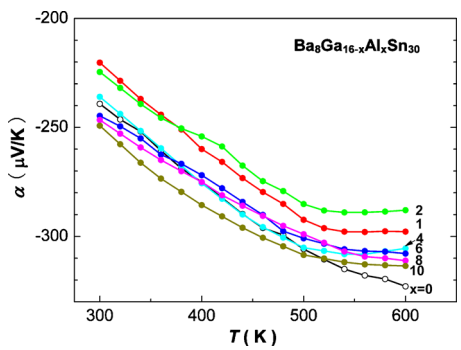

FIG. 5. (Color online) Temperature dependence of Seebeck coefficient α of type-VIII clathrate $Ba_8Ga_{16-x}Al_xSn_{30}$.

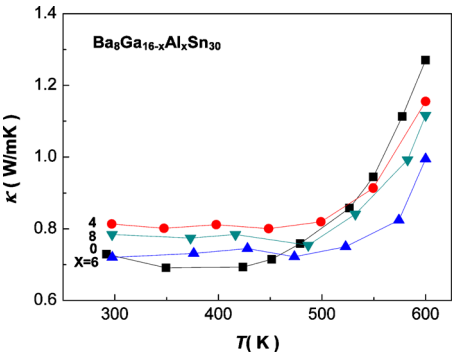

FIG. 7. (Color online) Temperature dependence of thermal conductivity κ for type-VIII clathrate $Ba_8Ga_{16-x}Al_xSn_{30}$.

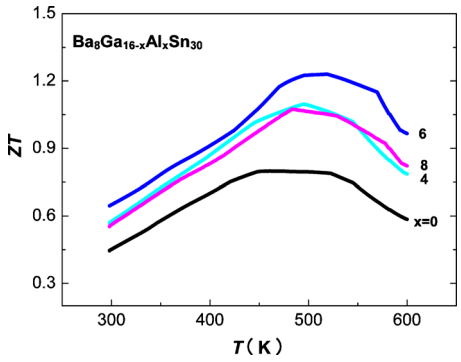

FIG. 8. (Color online) Temperature dependence of dimensionless figure of merit *ZT* for type-VIII clathrate $Ba_8Ga_{16-x}Al_xSn_{30}$.

culated for the four samples. As shown in Fig. 8, the maximum value of *ZT* for $x=6$ reaches 1.2 at 500 K.

IV. CONCLUSIONS

We have grown single-crystalline samples of type-VIII clathrate $Ba_8Ga_{16-x}Al_xSn_{30}$ $(0 \leq x \leq 12)$ with *n*-type carriers by Sn-flux method. The lattice parameter at room temperature increases linearly by 0.5% as the crystal composition of Al is increased to 10.5, which is the solubility limit. The TE properties were studied from 300 to 600 K. The Seebeck coefficients of all samples are largely negative. Although the carrier density hardly changes with *x*, the electrical resistivity for $1 \leq x \leq 6$ is reduced to 70% of that for $x=0$. The κ of samples with $x=0$ and 6 stays at rather low value of 0.72 W/mK up to 480 K. As a result, the highest $ZT=1.2$ is achieved at 500 K for $x=6$. Thus, this material system without toxic elements is proved to have high potential for application at temperatures from 400 to 600 K. Further improvement may be possible by controlling the starting compositions of Al and Sn. The lower price and lighter in weight of Al than Ga would become advantage for application to recover waste heat at intermediate temperatures from automobiles and industrial furnaces.

ACKNOWLEDGMENTS

We would like to thank Y. Kono, N. Ohya, and T. Taguchi for thermal conductivity measurements, and Y. Shibata for EPMA performed at Natural Science Center for Basic Research and Development, Hiroshima University. We acknowledge K. Akai for valuable discussion. This work was supported by New Energy and Industrial Technology Development Organization (NEDO, Grant No. 09002139-0) and Grant-in-Aid for Scientific Research from MEXT of Japan, Grants No. 1824032, No. 19051011, and No. 20102004.

[1] G. S. Nolas, J. L. Cohn, G. A. Slack, and S. B. Schujman, Appl. Phys. Lett. **73**, 178 (1998).
[2] V. L. Kuznetsov, L. A. Kuznetsova, A. E. Kaliazin, and D. M. Rowe, J. Appl. Phys. **87**, 7871 (2000).
[3] A. Saramat, G. Svensson, A. E. C. Palmqvist, C. Stiewe, E. Mueller, D. Platzek, S. G. K. Williams, D. M. Rowe, J. D. Bryan, and G. D. Stucky, J. Appl. Phys. **99**, 023708 (2006).
[4] J. H. Kim, N. L. Okamoto, K. Kishida, K. Tanaka, and H. Inui, Acta Mater. **54**, 2057 (2006).
[5] J. L. Cohn, G. S. Nolas, V. Fessatidis, T. H. Metcalf, and G. A. Slack, Phys. Rev. Lett. **82**, 779 (1999).
[6] A. Bentien, V. Pacheco, S. Paschen, Yu. Grin, and F. Steglich, Phys. Rev. B **71**, 165206 (2005).
[7] K. F. Cai, L. C. Zhang, Q. Lei, E. Müller, and C. Stiewe, Cryst. Growth Des. **6**, 1797 (2006).
[8] J. D. Bryan, N. P. Blake, H. Metiu, B. B. Iversen, R. D. Poulsen, and A. Bentien, J. Appl. Phys. **92**, 7281 (2002).
[9] N. L. Okamoto, K. Kishida, K. Tanaka, and H. Inui, J. Appl. Phys. **100**, 073504 (2006).
[10] M. Kozina, F. Bridges, Y. Jiang, M. A. Avila, K. Suekuni, and T. Takabatake, Phys. Rev. B **80**, 212101 (2009).
[11] J. Nicolas, G. Pierre, P Stanislas, C. Bernard, M. Michel, D. Patrice, D. Rodolphe, G. Graziella, C. Christian, and P. Michel, C. R. Chimie **8**, 39 (2005).
[12] F. May, E. S. Toberer, A. Saramat, and G. J. Snyder, Phys. Rev. B **80**, 125205 (2009).
[13] J. Martin, G. S. Nolas, H. Wang, and J. Yang, J. Appl. Phys. **102**, 103719 (2007).
[14] S. Latturner, X. Bu, N. Blake, H. Metiu, and G. Stucky, J. Solid State Chem. **151**, 61 (2000).
[15] T. Matsui, J. Furukawa, K. Tsukamoto, H. Tsuda, and K. Morii, J. Alloys Compd. **391**, 284 (2005).
[16] S. Paschen, W. Carrillo-Cabrera, A. Bentien, V. H. Tran, M. Baenitz, Y. Grin, and F. Steglich, Phys. Rev. B **64**, 214404 (2001).
[17] Y. Sasaki, K. Kishimoto, T. Koyanagi, H. Asada, and K. Akai, J. Appl. Phys. **105**, 073702 (2009).
[18] K. Kishimoto, N. Ikeda, K. Akai, and T. Koyanagi, Appl. Phys. Express **1**, 031201 (2008).
[19] M. A. Avila, K. Suekuni, K. Umeo, and T. Takabatake, Physica B **383**, 124 (2006).
[20] K. Suekuni, M. A. Avila, K. Umeo, H. Fukuoka, S. Yamanaka, T. Nakagawa, and T. Takabatake, Phys. Rev. B **77**, 235119 (2008).
[21] D. Huo, T. Sakata, T. Sasakawa, M. A. Avila, M. Tsubota, F. Iga, H. Fukuoka, S. Yamanaka, S. Aoyagi, and T. Takabatake, Phys. Rev. B **71**, 075113 (2005).
[22] G. S. Nolas, J. L. Cohn, J. S. Dyck, C. Uher, G. A. Lamberton, Jr., and T. M. Tritt, J. Mater. Res. **19**, 3556 (2004).
[23] M. H. Phan, G. T. Woods, A. Chaturvedi, S. Stefanoski, G. S. Nolas, and H. Srikant, Appl. Phys. Lett. **93**, 252505 (2008).
[24] V. Pacheco, A. Bentien, W. Carrillo-Cabrera, S. Paschen, F. Steglich, and Yu. Grin, Phys. Rev. B **71**, 165205 (2005).
[25] H. J. Goldsmid, *Introduction to Thermoelectricity* (Springer, Berlin, 2010).